TKEO-DESA-Based Decision Tree for Power Quality Events Detection and Classification

J. L. Montalvo, J.C. Silva, and Alejandro Zamora-Mendez

***Abstract*—This paper proposes a novel strategy to detect and classify power quality disturbances. The strategy comprises the Teager-Kaiser energy operator (TKEO) and the discrete energy separation algorithm (DESA). The TKEO is used to track the signal energy and capture the energy changes, whereas the DESA algorithm is utilized to estimate the frequency and amplitude of the signal. These features are employed to build a ruled decision tree to detect and classify 15 PQ disturbances. PQ events with a complex nature are generated given the IEEE-1159 standard by PQ-SyDa toolbox. To confirm the effectiveness and performance of the proposed strategy, it is evaluated using synthetic signals, time-domain simulations performed in Matlab/Simulink, and real sag events where an accuracy prediction of around 97% is reached.**

***Keywords*—Classification, detection, discrete energy separation algorithm, power quality disturbances, ruled decision tree, Teager-Kaiser energy operator.**

I. Introduction

Nowadays, the micro-generation systems integration, switching of capacitor banks, presence of nonlinear loads, input and output of large inductive loads, faults in the primary distribution feeder, lightning, and the power electronics equipment increase and their sensitive components to supply fluctuations, among other factors are caused by the power quality assessment importance [1], [2], [3], [4].

To ensure power quality adequate level, it is necessary to identify and classify the PQ events correctly. PQ events are described in the IEEE 1159 standard, which depends on their time-varying statistical characteristics [5], [6]. On the other hand, the PQ measurement methods to achieve the information to obtain the class of an event and their parameters are reported in the IEC61000-4-30 standard [7].

The detection and classification of power quality disturbances have been meanly addressed by two approaches: signal processing techniques and the application of pattern recognition techniques [8], [9], [10], [11]. The former focuses on feature extraction techniques such as Fourier transform, S transform, Hilbert Huang transform, Wavelet transform, and miscellaneous feature extraction techniques [8], [9], [10], [11]. The latter is based on machine learning-based classification techniques such as Support Vector Machine, Artificial Neural Network, Fuzzy Logic, Neuro-Fuzzy, Genetic algorithms, and Deep learning classification methods [8], [9], [10], [11].

Into the signal processing-based feature extraction techniques are included the short-time Fourier transform (STFT) [12], and the Gabor transform (GT) [13], which provides phase and frequency information, but exhibits inadequate temporal resolution and susceptibility to long-term problems. The wavelet transform (WT) results in a suitable tool for discontinuous and suddenly changing signals, and also presents usefulness in identifying events such as sags, swell, over-voltage, flickers, power interruption, electrical noise, and harmonic distortion. However, it presents degraded phase information in noisy conditions [14], [15], [16], [17]. The Stockwell transform (ST) improves the adaptive time-frequency resolution but at a high computational cost [18].

Conversely, adaptive mode decomposition methods have gained popularity due to their highly adaptive capabilities and data-driven nature. For instance, the empirical mode decomposition (EMD) is a method that decomposes complex signals into intrinsic mode functions and adaptive time-frequency decomposition, but exhibits limited decomposition performance due to mode mixing and endpoint effect [19]. On the other hand, the features of the Hilbert Huang transform (HHT) are based on instantaneous time and frequency extracted with basic EMD building blocks, however, it presents a misidentification in the frequency signal that introduces distortion [20]. Furthermore, variational mode decomposition (VMD) aims to decompose a complex signal into a number of user-defined modes but presents limited decomposition performance due to abrupt signal onset and endpoint effect [21]. Another adaptive and data-driven method similar to the EMD is the intrinsic time-scale decomposition (ITD) that offers flexibility and adaptability to capture the underlying features of complex non-stationary and non-linear signals [22]. Alternatively, the extended Kalman filter (EKF) is one method that presents less computation time without signal segmentation and feature selection step but presents errors due to a mismatch of signals and filter model [23]. Furthermore, Refs. [8], [9], [10], [11] provide a comprehensive summary of power quality disturbance detection and classification methods.

A. Contribution

The novelty of this investigation lies in the signal-processing technique (STP) based on the Teager-Kaiser energy operator

Authors from the Universidad Michoacana acknowledge the support provided by CONAHCYT through Project CF-2023-I-1174 within the framework of the "Ciencia de Frontera 2023". J. L. Montalvo is with the Master of Science Program in Electrical Engineering at the Michoacan University of Saint Nicholas of Hidalgo (UMSNH), Morelia 58030, México, (e-mail: 1614896g@umich.mx) J. C. Silva and A. Zamora are with the Electrical Engineering Faculty at the Michoacan University of Saint Nicholas of Hidalgo (UMSNH), Morelia, Michoacan 58030, Mexico, (e-mail: juan.silva@umich.mx), (e-mail of corresponding author: azamoram@umich.mx).

Paper submitted to the International Conference on Power Systems Transients (IPST2025) in Guadalajara, Mexico, June 8-12, 2025.

(TKEO) and the discrete energy separation algorithm (DESA) for feature extraction to detect and classify PQ disturbances. The second-order discrete-time Teager-Kaiser energy operator [24] to track the signal energy is used in the detection stage. Subsequently, the discrete energy separation algorithm [25] to extract the features of frequency and amplitude for a signal is used to classify the PQ event. In this way, the combination of the TKEO and DESA techniques is utilized to build a decision tree that allows the detection and classification of 15 different types of PQ disturbance signals. The potential and effectiveness of the proposed strategy (TKEO-DESA-based decision tree) are unveiled and tested under synthetic, simulated, and real data environments. Finally, our proposal exposes an accuracy prediction of around 97%.

Furthermore, compared to other approaches in the literature, the proposed technique has the advantage of being able to compute a signal's energy, frequency, and amplitude using three continuous samples. This allows a simple algorithm implementation using these three main features to build a decision tree to detect and classify PQ events.

II. Discrete Energy Separation Algorithm based on Teager-Kaiser Energy Operator

The Teager-Kaiser energy operator (TKEO) is a nonlinear energy operator for continuous-time and discrete-time signals that was developed by Teager [26] and subsequently introduced systematically by Kaiser [24]. The TKEO is highly effective for numerous applications including the development of the energy separation algorithm (ESA) for demodulating AM-FM signals, tracking speech modulations, detecting events in non-stationary signals [27], and power systems applications [28], [29], [30].

In this paper, the TKEO with its discrete-time energy operator and the discrete energy separation algorithm (DESA), which provides instantaneous frequency and amplitude estimates, are used to detect and classify power quality events.

A. Discrete-time Teager-Kaiser Energy Operator

The second-order operator is introduced by Kaiser where it is started by a second-order differential equation that describes Newton's law of motion applied to a mass m suspended by a spring of force constant k as can be seen in (1) [24].

$$\ddot{x} + \frac{k}{m}x = 0 \tag{1}$$

So, the solution of (1) is given by $x(t) = Acos(\omega t + \phi)$ that corresponds to the displacement produced by a mass-spring undamped linear oscillator, where A and $\omega = \sqrt{k/m}$ are the amplitude and frequency of the oscillation, respectively, and ϕ is the initial phase [24]. Thus, the total energy E of the system is given by the sum of the potential energy of the spring and the kinetic energy of the object [24]:

$$\begin{aligned} \frac{1}{2}(kx^2 + m\dot{x}^2) =& \frac{1}{2}mA^2\omega^2 \\ E \propto& A^2\omega^2 \end{aligned} \tag{2}$$

where the right side in (2) is for the solution x when this is substituted in E.

Then, for the discrete operator, let $x(n)$ be a digital signal described by [24]

$$x(n) = A\cos(\Omega n + \phi) \tag{3}$$

where $\Omega = \omega T$ and T denotes the sampling period, and let $x(n-1)$ and $x(n+1)$ two equally-spaced samples signals of x(n) as shown in (4) [24].

$$\begin{aligned} x(n-1) =& A\cos(\Omega(n+1) + \phi) \\ x(n+1) =& A\cos(\Omega(n-1) + \phi). \end{aligned} \tag{4}$$

Now, with the aid of the trigonometric identities given by

$$\begin{aligned} \cos\alpha\cos\beta =& \frac{1}{2}[\cos(\alpha-\beta) + \cos(\alpha+\beta)] \\ \cos(2\alpha) =& 1 - 2\sin^2\alpha \end{aligned} \tag{5}$$

equation (4) results in [24]

$$x(n+1)x(n-1) = A^2\cos^2(\Omega n + \phi) - A^2\sin^2(\Omega) \tag{6}$$

where is evident that $A^2\cos^2(\Omega n + \phi) = x^2(n)$. Therefore,

$$A^2\sin^2(\Omega) = x^2(n) - x(n+1)x(n-1). \tag{7}$$

for small values of Ω, $\sin\Omega \approx \Omega$. Thus, the discrete-time energy operator for the second order to track the energy is expressed by [24], [25], [26], [27]:

$$E(n) = \Psi[x(n)] = x^2(n) - x(n+1)x(n-1) \tag{8}$$

where $E(n) = \Psi[x(n)] = A^2\sin^2(\Omega) \approx A^2\Omega^2$.

B. Discrete-time energy separation algorithm

For the discrete-time energy separation algorithm (DESA), consider the first derivative of $x(n)$ using two-sample backward difference approximation as [25]:

$$y(n) = x(n) - x(n-1). \tag{9}$$

Thus, applying the discrete energy operator to the first derivative described by (9) becomes [25]:

$$\Psi[y(n)] = 4A^2\sin^2(\Omega/2)\sin^2\Omega \tag{10}$$

So, the expression in (10) may be combined with (7) and used to obtain the following expression:

$$\frac{\Psi[y(n)]}{2\Psi[x(n)]} = 2\sin^2(\Omega/2) = 1 - \cos(\Omega) \tag{11}$$

Now, considering the above expressions, the DESA allows us to obtain the energy operator and separate the output energy product to estimate the instantaneous frequency and amplitude [25].

$$\Omega(n) \approx \arccos\left(1 - \frac{\Psi[y(n)]}{2\Psi[x(n)]}\right) \tag{12}$$

$$A(n) \approx \sqrt{\frac{\Psi[x(n)]}{1 - \left(1 - \frac{\Psi[y(n)]}{2\Psi[x(n)]}\right)^2}} \tag{13}$$

III. Proposed Methodology for PQ Events Detection and Classification

The proposed methodology for the detection and classification of power quality events based on the Teager-Kaiser energy operator and the discrete energy separation algorithm is described in this Section. For the proposed approach, PQ disturbances are synthetically generated using the Power Quality Synthetic Disturbances DataSet toolbox (PQ-SyDa) [31]. This toolbox is based on the IEEE standard 1159 [6] and is available in [32]. Also, 29 different PQ event datasets can be generated. Then, the proposal methodology is able to classify 15 of the 29 types of different PQ disturbances generated by PQ-SyDa and are presented in Table I.

TABLE I
PQ TEST SIGNALS AND THEIR LABELS

Signal	Label	Signal	Label
Pure Signal	M1	Harmonics with Swell	M9
Sag	M2	Flicker	M10
Swell	M3	Flicker with Sag	M11
Interruption	M4	Flicker with Swell	M12
Peak/Impulse	M5	Sag with Harmonics	M13
Oscillatory Transient	M6	Swell with Harmonics	M14
Harmonics	M7	Notch	M15
Harmonics with Sag	M8		

The flowchart for the TKEO-DESA methodology to detect and classify PQ disturbances is illustrated in Fig. 1.

According to Fig. 1, the input signal should be in PU to define the thresholds of the proposal and keep them to the same values for any input signal. In addition, a 9-cycle analysis window is used.

So, to describe the proposal methodology a test signal is used. This test signal corresponds to a synthetic sag signal labelled M2 (see Table I) and is generated by PQ-SyDa as shown in Fig. 2(a). For all synthetic signals, a 7680 Hz sampling frequency is used, considering a 60 Hz nominal frequency. Thus, for the second step of Fig. 1, the TKEO and DESA algorithms are applied to the input signal through (8), (12)-(13), respectively. So, with the Teager-Kaiser energy operator, $E(n)$, the signal energy can be tracked. This allows us to detect the disturbance using the change in the energy ΔE_i presented in the signal. In this way, for the test signal with sag, the TKEO is able to detect two energy changes ΔE_1 and ΔE_2, that is, when the disturbance starts and when the disturbance stops. This is shown in Fig. 2(b) and is indicated by the two red circles. Likewise, this allows us to know the duration of the disturbance, which is denoted as t_d. Besides that, the analysis window can be split into three subwindows using these two points. The first subwindow contains the samples before the event and is denoted as be, the second subwindow incorporates the event duration samples and is represented by ed, and finally, the third subwindow is composed of the after-event samples and is symbolised as ae. These variables are depicted in Figs. 1 and 2(b) as be, ed, and ae, respectively.

Now, for the classification of power quality disturbances, a DESA-based decision tree is used as shown in Fig. 3.

So, for the decision tree based on the TKEO and DESA methods, additional feature extraction from PQ events of both the actual signal and its amplitude and frequency are used to classify the PQ disturbances. These extracted features consist of the peak-to-peak value and the mean value as shown in (14) and (15), respectively.

$$f_d = f_{max} - f_{min} \tag{14}$$

$$f_m = \frac{1}{N}\sum_{1}^{N} f(n) \tag{15}$$

where f can represent the actual signal $x(n)$, its frequency $\Omega(n)$, or its amplitude $A(n)$, which are described by (3), (12), and (13), respectively. So, f_d and f_m denote the peak-to-peak and mean values, respectively, whether for the actual signal, its frequency, or its amplitude. Besides, N is the number of samples for a corresponding analysis window or subwindow. In this way, f_d and f_m can be applied to the three subwindows getting $x_d(ed)$, $A_m(be)$, $A_m(ed)$, $A_m(ae)$, $A_d(be)$, $\Omega_d(ed)$, $\Omega_m(be)$, $\Omega_m(ed)$, and $\Omega_m(ae)$. Also, we can get x_m, A_m, and Ω_d when (14) and (15) are applied for the complete analysis

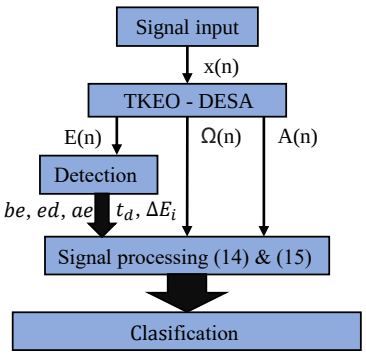

Fig. 1. General flowchart for the TKEO-DESA methodology to detect and classify PQ disturbances.

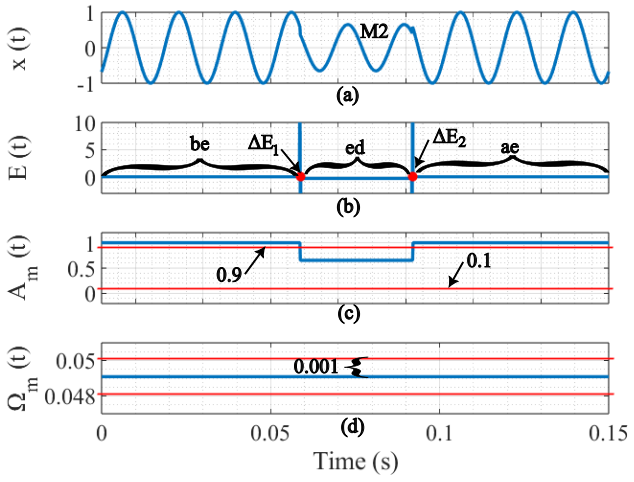

Fig. 2. (a) Signal with sag. (b) TKEO. (c) Amplitude mean value. (d) Frequency mean value.

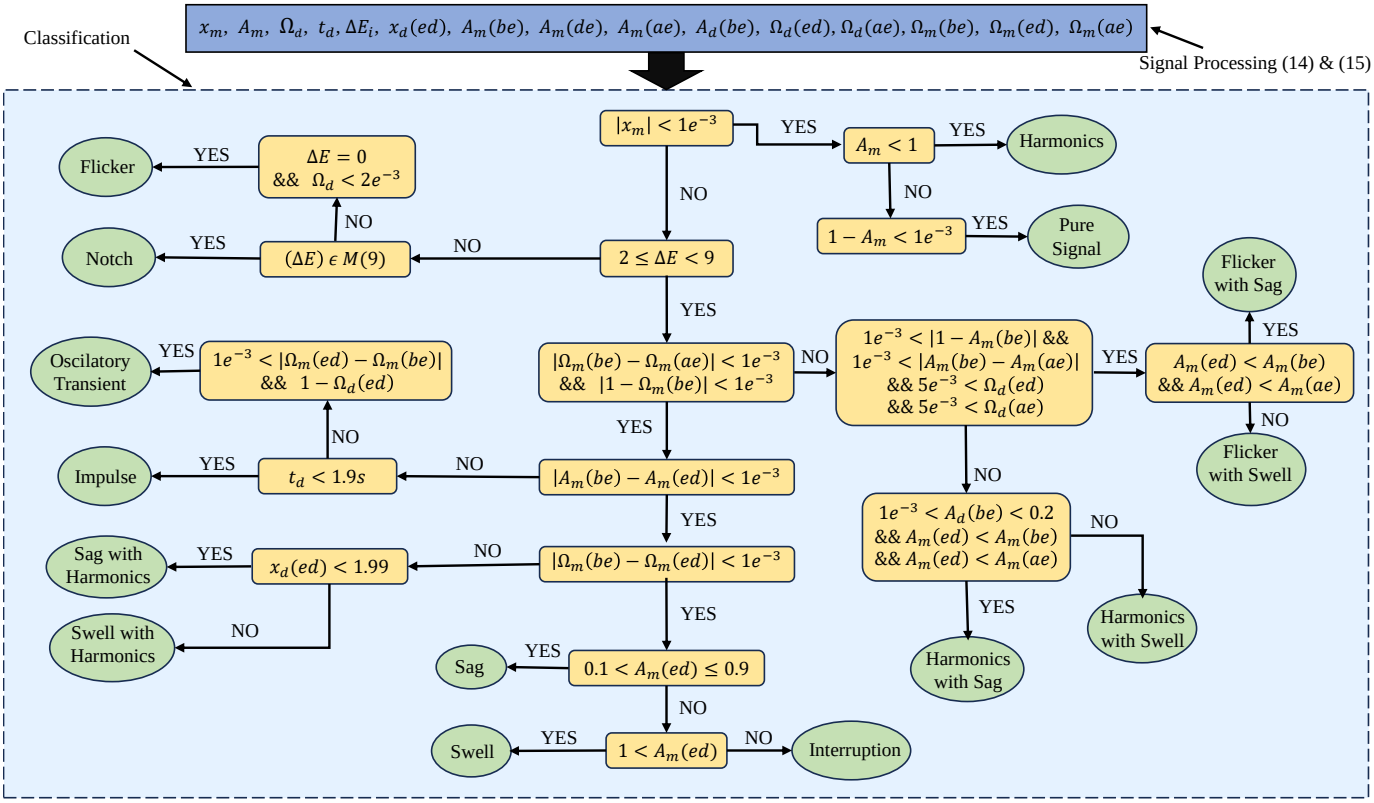

Fig. 3. TKEO-DESA-based decision tree for PQ events classification.

window. These features are used for the decision tree in the PQ disturbances classification as shown in Fig. 3.

Then, for the test signal, the most important features are A_m and Ω_m measurements as illustrated in Figs. 2(c) and 2(d), respectively. Notice that A_m signal is into the threshold shown in the decision-tree flowchart, ie, between 0.1 and 0.9. On the other hand, Ω_m is less than $1e^{-3}$, so, following the decision tree, the test signal is classified as a sag, i.e., M2 label. With the proposed TKEO-DESA-based decision tree, the classifier can classify 15 PQ disturbances using the input signal and its amplitude and frequency features.

TABLE II
TKEO-DESA-BASED DECISION TREE CLASSIFICATION RESULTS FOR PQ DISTURBANCES

Signal	Accuracy (%)	Signal	Accuracy (%)
Pure Signal	100	Harmonics with Swell	98.2
Sag	98	Flicker	95.4
Swell	97.8	Flicker with Sag	97
Interruption	98.2	Flicker with Swell	97
Impulse	98.2	Sag with Harmonics	96
Oscillatory Transient	96	Swell with Harmonics	96
Harmonics	94	Notch	95
Harmonics with Sag	99.2	Overall accuracy	97.03

IV. RESULTS AND VALIDATION FOR THE PROPOSED METHODOLOGY

To validate the applicability of the proposal three test cases are described in the following: (*i*) theoretical PQ disturbances generated by PQ-SyDa, (*ii*) simulated signals by simulink cases, and (*iii*) real-life power quality sags.

A. Application on theoretical PQ disturbances

To test the proposal with synthetic PQ disturbances the PQ-SyDa is used to generate 100 random events for each disturbance presented in Table I. Table II shows the accuracy results for the 15 PQ disturbances. Notice that the proposal methodology has a 99.2% for the harmonics with sag signal and a 94% for the harmonics signal, with an overall accuracy of 97.03%.

For instance, Fig. 4 illustrates the results for a harmonics with sag synthetic case. Notice that the proposal is able to detect and identify the PQ disturbance as an M8 label, i.e., harmonics with sag according to Table I. For the decision tree, Fig. 4(b) depicts the signal energy tracked by the TKEO where two energy changes are detected. This lets us know the number of samples for each subwindow and classify the event. In this way, Figs. 4(c) and 4(d) show the most important features to carry out the classification which are A_m and Ω_m, respectively. Besides, the thresholds presented in the decision tree of Fig. 3, also are illustrated in Figs. 4(c) and 4(d) indicate that the PQ disturbance corresponds to harmonics with sag disturbance.

For comparison purposes, Table III depicts the accuracy of different techniques used for PQ event detection and classification in the literature; for more detail, please see Table 6 from ref. [33]. For that, the number of complex PQ disturbances and the number of features are taken into account,

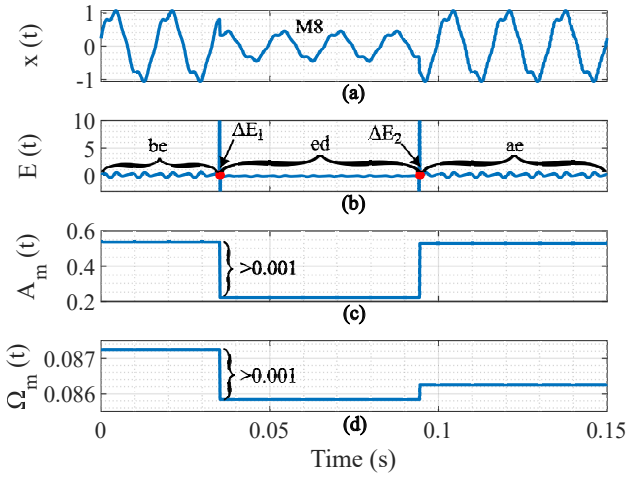

Fig. 4. (a) Harmonics with sag signal, (b) TKEO, (c) Amplitude mean value, (d) Frequency mean value.

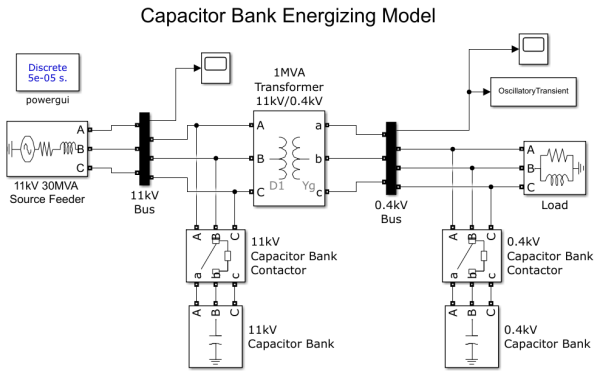

Fig. 5. Simulation of a capacitor bank energizing [37].

where complex means that multiple PQ events appear. So, for the proposal method, just the complex PQ disturbances presented in Table I are considered in Table III. Notice that the proposed algorithm used fewer features compared to the methods presented in Table III reaching an accuracy of around 97%.

TABLE III
COMPARISON AMONG DIFFERENT WORKS FOR PQ EVENTS DETECTION AND CLASSIFICATION

Ref.	Technique	Number of Complex PQ Events	Number of features	Overall Accuracy (%)
[34]	ST+APSO	4	6	96.5
[35]	DWT + WNs	6	8	97.5
[36]	Spline WT+ST	3	8	97
[33]	ST+FES	6	7	98.7
Proposed	TKEO-DESA	6	4	97

B. Application on power quality disturbances simulation

This section applies the proposed methodology to two simulated signals obtained from MATLAB/Simulink models [37]. The first model is a capacitor bank energization to simulate a voltage oscillatory transient and is presented in Fig. 5. According to [37], the model contains a three-phase source of 11 kV, 30 MVA, 60 Hz that feeds an 11 kV/0.4 kV, 1 MVA delta/wye transformer to a 100 kW and 100 kvar resistive and inductive loads, respectively. The capacitor bank at 0.4 kV bus is 40 kvar, whereas, the capacitor bank at 11 kV bus is 100 kvar.

To validate the applicability of the proposal, the test signal is obtained from a 0.4 kV bus (see Fig. 5) and is shown in Fig. 6(a). Figure 6(b) illustrates the phase a in p.u. for testing the proposal where the classification is labeled as M6, corresponding to Table I as an oscillatory transient. For the decision tree, Fig. 6(c) depicts the signal energy where two energy changes are detected. Notice that these two points

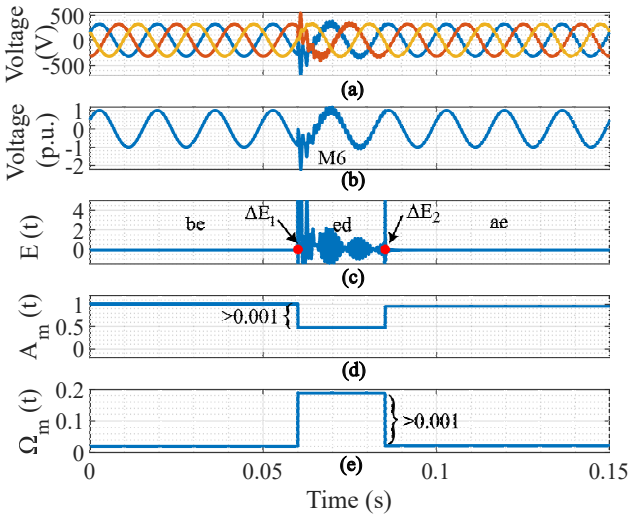

Fig. 6. (a) Voltages at 0.4 kV bus. (b) Phase a to be analysed in p.u. (c) TKEO of phase a. (d) Amplitude mean value. (e) Frequency mean value.

clearly limited the event in time. Finally, Figs. 6(d) and 6(e) illustrate the two main features with which the event can be classified showing that both measurements exceed the thresholds proposed in the decision tree of Fig. 3.

For the second simulated model, a single-phase nonlinear load is used and is shown in Fig. 7 [37]. This model simulates a harmonic voltage disturbance caused by a single-phase bridge rectifier common for domestic and commercial buildings. According to [37], the model contains an 11 kV, 30 MVA, 60 Hz three-phase source to feed an 11 kV/0.4 kV, 1 MVA delta/wye transformer to a 1 MW resistive load.

Figure 8(a) depicts the three-phase signals obtained from the 0.4 kV bus of the Simulink model in Fig.7. So, phase a in p.u. is used to test the proposal and is shown in Fig. 8(b) where the proposed methodology classifies the test signal as harmonics, i.e., M7 label of Table I. For the decision tree, the main feature is the instantaneous amplitude which is depicted in Fig. 8(c) being less than 1, which classifies the event as harmonic, according to Fig. 3.

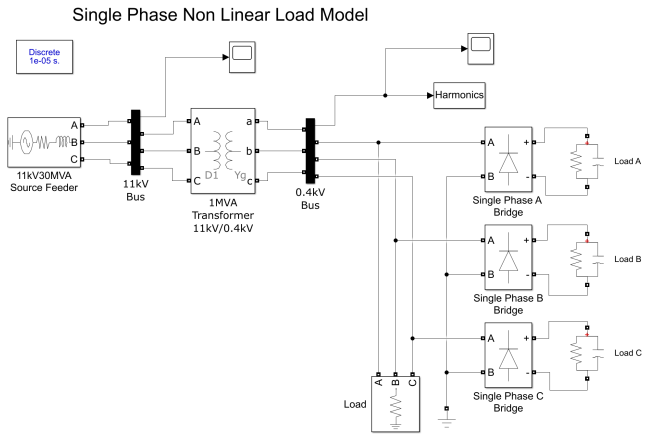

Fig. 7. Single-phase nonlinear load model [37].

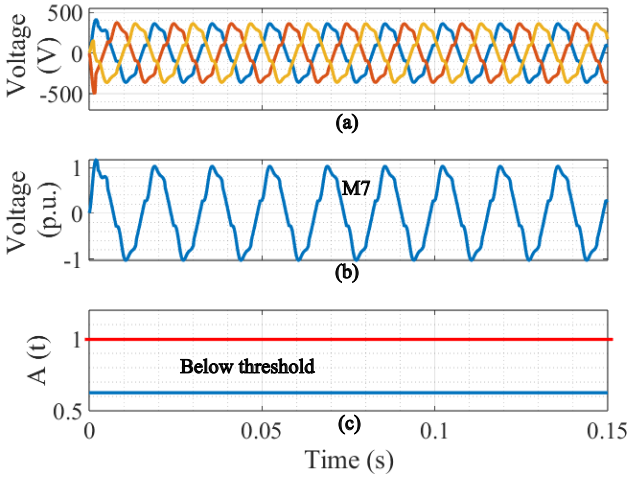

Fig. 8. (a) Harmonic voltages at 0.4 kV bus. (b) Phase a to be analyzed in p.u. (c) Instantaneous amplitude.

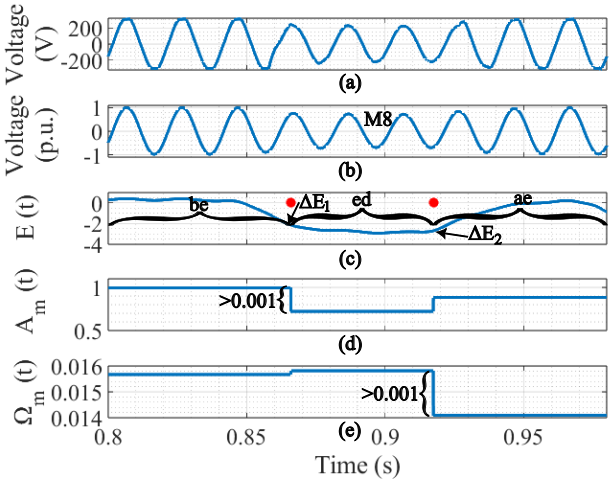

Fig. 9. (a) First real sag event. (b) First real sag event in p.u. after the Butterworth filter is applied. (c) TKEO, (d) Amplitude mean value, (e) Frequency mean value.

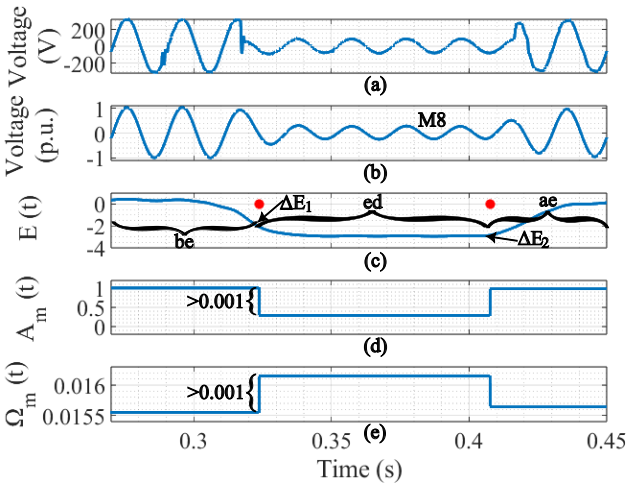

Fig. 10. (a) Second real sag event. (b) Second real sag event in p.u. after the Butterworth filter is applied. (c) TKEO, (d) Amplitude mean value, (e) Frequency mean value.

C. Application on real power quality sags

The proposed methodology is also applied to detect and classify real-life sag events. The dataset employed is available in [38] and provides signal recordings from the power network of the University of Cadiz during the last five years (electrical network according to the UNE-EN-50160: 2011 [38]). The signals have been designed from the basis of representative single-isolated events for a 50Hz network with a sampling frequency of 20 kHz (400 samples per cycle) [38]. To demonstrate the effectiveness of the methodology, two random real sag events are chosen from the dataset in [38] where a second-order low-pass filter type Butterworth (360 Hz cut-off frequency) is used as an anti-aliasing filter. As a result, Figs. 9(a) and 10(b) show the two real sag events before and after the Butterworth filter is applied. Notice that the signals are also converted to p.u. So, the TKEO-DESA-based decision tree classified the disturbance as harmonic with sag according to Table I, i.e., M8 label. It is important to mention, that since even at first glance it seems that the signal is free of harmonics, when it is observed in more detail, the signal contains noise and harmonic content, and since it is not a pure signal, the decision tree classifies as a harmonic with sag. Thus, the classification of this event is the same as shown in Fig. 4.

Finally, the second real sag disturbance is shown in Fig. 10(a). So, similarly to the previous real sag case, the TKEO-DESA-based decision tree classified the disturbance as harmonic with sag, i.e., M8 label as can be seen in Fig. 10(b). The main features are illustrated in Figs. 10(c)-(d) which are similar to the Fig. 4.

V. Conclusions

This paper has successfully demonstrated that a new strategy based on a signal-processing technique for feature extraction can appropriately detect and classify 15 power quality disturbances. The proposed methodology used the

Teager-Kaiser energy operator and the discrete energy separation algorithm to build a ruled decision tree strategy to detect and classify PQ disturbances. The TKEO is applied to track the signal energy and in this way, detect the energy changes. Furthermore, the frequency and amplitude of the signal can be obtained using the DESA algorithm. Thereby, a TKEO-DESA-based ruled decision tree is built that allows us to detect and classify PQ events using the features obtained by these algorithms. Moreover, its easy implementation and the fixed window of 9 cycles make it suitable for possible real-time applications.

REFERENCES

[1] A. M. Gargoom, N. Ertugrul, and W. L. Soong, "Automatic classification and characterization of power quality events," *IEEE Transactions on Power Delivery*, vol. 23, no. 4, pp. 2417–2425, 2008.

[2] D. Singh, A. Chandra, and K. Al-Haddad *Power Quality: Problems and Mitigation Techniques; Influence of harmonics on power distribution system protection*, 2015.

[3] H. Shao, R. Henriques, H. Morais, and E. Tedeschi, "Power quality monitoring in electric grid integrating offshore wind energy: A review," *Renewable and Sustainable Energy Reviews*, vol. 191, p. 114094, 03 2024.

[4] F. Borges, R. Fernandes, I. Silva, and C. Silva, "Feature extraction and power quality disturbances classification using smart meters," *IEEE Transactions on Industrial Informatics*, vol. 12, pp. 1–1, 01 2015.

[5] B. Biswal, P. Dash, and B. Panigrahi, "Non-stationary power signal processing for pattern recognition using hs-transform," *Applied Soft Computing*, vol. 9, no. 1, pp. 107–117, 2009.

[6] "Ieee recommended practice for monitoring electric power quality," *IEEE Std 1159-2019 (Revision of IEEE Std 1159-2009)*, pp. 1–98, 2019.

[7] "Testing and measurement techniques—power quality measurement methods," *IEC 61000-4-30*, pp. 1–98, 2021.

[8] Z. Oubrahim, Y. Amirat, M. Benbouzid, and M. Ouassaid, "Power quality disturbances characterization using signal processing and pattern recognition techniques: A comprehensive review," *Energies*, vol. 16, no. 6, 2023.

[9] P. Khetarpal and M. M. Tripathi, "A critical and comprehensive review on power quality disturbance detection and classification," *Sustainable Computing: Informatics and Systems*, vol. 28, p. 100417, 2020.

[10] M. Mishra, "Power quality disturbance detection and classification using signal processing and soft computing techniques: A comprehensive review," *International Transactions on Electrical Energy Systems*, vol. 29, no. 8, p. e12008, 2019. e12008 ITEES-18-0827.R2.

[11] G. S. Chawda, A. G. Shaik, M. Shaik, S. Padmanaban, J. B. Holm-Nielsen, O. P. Mahela, and P. Kaliannan, "Comprehensive review on detection and classification of power quality disturbances in utility grid with renewable energy penetration," *IEEE Access*, vol. 8, pp. 146807–146830, 2020.

[12] K. Satpathi, Y. M. Yeap, A. Ukil, and N. Geddada, "Short-time fourier transform based transient analysis of vsc interfaced point-to-point dc system," *IEEE Transactions on Industrial Electronics*, vol. 65, pp. 4080 – 4091, 05 2018.

[13] A. Salemnia and S. Naderian, "A new method for classification of power quality events based on discrete gabor transform with fir window and type-2 fuzzy kernel-based svm and its experimental verification," *IET Generation, Transmission & Distribution*, vol. 11, 09 2016.

[14] K. Thirumala, M. Prasad, T. Jain, and A. Umarikar, "Tunable - q wavelet transform and dual multi-class svm for online automatic detection of power quality disturbances," *IEEE Transactions on Smart Grid*, vol. 9, pp. 3018 – 3028, 07 2018.

[15] R. Salles and P. Ribeiro, "The use of deep learning and 2-d wavelet scalograms for power quality disturbances classification," *Electric Power Systems Research*, vol. 214, p. 108834, 10 2022.

[16] E. Nagata, D. Ferreira, M. Bollen, B. Barbosa, E. Ribeiro, C. Duque, and P. Ribeiro, "Real-time voltage sag detection and classification for power quality diagnostics," *Measurement*, vol. 164, p. 108097, 06 2020.

[17] Y. Mei, Y. Wang, X. Zhang, S. Liu, Q. Wei, and Z. Dou, "Wavelet packet transform and improved complete ensemble empirical mode decomposition with adaptive noise based power quality disturbance detection," *Journal of Power Electronics*, vol. 22, pp. 1334–1346, Aug. 2022.

[18] F. Zaro, "Power quality disturbances detection and classification rule-based decision tree," *WSEAS TRANSACTIONS ON SIGNAL PROCESSING*, vol. 17, pp. 22–27, 04 2021.

[19] H. Li, B. Yi, Q. Li, J. Ming, and Z. Zhao, "Evaluation of dc power quality based on empirical mode decomposition and one-dimensional convolutional neural network," *IEEE Access*, vol. PP, pp. 1–1, 02 2020.

[20] M. Sahani and P. K. Dash, "Automatic power quality events recognition based on hilbert huang transform and extreme learning machine," *IEEE Transactions on Industrial Informatics*, vol. PP, pp. 1–1, 02 2018.

[21] M. Alam, F. Bai, R. Yan, and T. Saha, "Classification and visualization of power quality disturbance-events using space vector ellipse in complex plane," *IEEE Transactions on Power Delivery*, vol. PP, pp. 1–1, 07 2020.

[22] K. Zhu, Z. Teng, W. Qiu, Q. Tang, and W. Yao, "Complex disturbances identification: A novel pqds decomposition and modeling method," *IEEE Transactions on Industrial Electronics*, vol. 70, no. 6, pp. 6356–6365, 2023.

[23] Y. Simhamed, F. Ykhlef, and A. Iratni, "A new classification scheme based on extended kalman filter and support vector machine," *Electric Power Systems Research*, vol. 210, p. 108153, 09 2022.

[24] J. Kaiser, "On a simple algorithm to calculate the 'energy' of a signal," in *International Conference on Acoustics, Speech, and Signal Processing*, pp. 381–384 vol.1, 1990.

[25] P. Maragos, J. F. Kaiser, and T. F. Quatieri, "Energy separation in signal modulations with application to speech analysis," *IEEE transactions on signal processing*, vol. 41, no. 10, pp. 3024–3051, 1993.

[26] H. M. Teager and S. M. Teager, "Evidence for nonlinear sound production mechanisms in the vocal tract," in *Speech Production and Modelling*, vol. 55, pp. 17–29, ser. NATO Advanced Study Institute Series D, W. J. Hardcastle and A. Marchal, Eds. Boston, MA: Kluwer, Jul 1989.

[27] P. Maragos, A. Potamianos, and B. Santhanam, "Instantaneous energy operators: Applications to speech processing and communications," *Proc. IEEE Workshop on Nonlinear Signal and Image Processing, Halkidiki, Greece*, june 1995.

[28] I. Kamwa, A. K. Pradhan, and G. Joós, "Robust detection and analysis of power system oscillations using the teager-kaiser energy operator," *IEEE Trans. Power Syst.*, vol. 26, no. 1, pp. 323–333, 2010.

[29] A. Zamora-Mendez, R. D. R. de Luna, J. A. de la O Serna, J. H. Chow, and M. R. A. Paternina, "Electromechanical modes identification based on an iterative eigenvalue decomposition of the hankel matrix," *IEEE Transactions on Power Systems*, vol. 38, no. 1, pp. 155–167, 2023.

[30] D. Rodales, A. Zamora-Mendez, J. A. de la O Serna, J. M. Ramirez, M. R. A. Paternina, L. Lugnani, G. E. Mejia-Ruiz, A. Sanchez-Ocampo, and D. Dotta, "Model-free inertia estimation in bulk power grids through o-splines," *International Journal of Electrical Power & Energy Systems*, vol. 153, p. 109323, 2023.

[31] M. Juarez, A. Zamora-Mendez, J. Ortiz-Bejar, J. C. Silva, J. Cerda, and M. Paternina, "Pq-syda: Power quality synthetic disturbances dataset," *2024 IEEE PES Generation, Transmission and Distribution Latin America Conference and Industrial Exposition (GTDLA). Ixtapa, Mexico*, p. Accepted, 2024.

[32] M. G. J. Jimenez, "Power quality synthetic disturbances dataset (pq-syda)," 2024. https://github.com/Micke1995/ROPEC-2024 [Accessed: (6/22/2024)].

[33] O. P. Mahela, A. G. Shaik, B. Khan, R. Mahla, and H. H. Alhelou, "Recognition of complex power quality disturbances using s-transform based ruled decision tree," *IEEE Access*, vol. 8, pp. 173530–173547, 2020.

[34] B. Biswal, P. K. Dash, and B. K. Panigrahi, "Power quality disturbance classification using fuzzy c-means algorithm and adaptive particle swarm optimization," *IEEE Transactions on Industrial Electronics*, vol. 56, no. 1, pp. 212–220, 2009.

[35] M. A. S. Masoum, S. Jamali, and N. Ghaffarzadeh, "Detection and classification of power quality disturbances using discrete wavelet transform and wavelet networks," *Iet Science Measurement & Technology*, vol. 4, pp. 193–205, 2010.

[36] P. Dash, B. Panigrahi, D. Sahoo, and G. Panda, "Power quality disturbance data compression, detection, and classification using integrated spline wavelet and s-transform," *IEEE Transactions on Power Delivery*, vol. 18, no. 2, pp. 595–600, 2003.

[37] R. H. Tan and V. K. Ramachandaramurthy, "A comprehensive modeling and simulation of power quality disturbances using matlab/simulink," in *Power Quality Issues in Distributed Generation* (J. Luszcz, ed.), ch. 3, Rijeka: IntechOpen, 2015.

[38] "Real-life power quality sags." https://dx.doi.org/10.21227/H2K88D, 2017.